



Article

Antimicrobial Activity of Fungal Endophytes Associated with *Peperomia argyreia* (Piperaceae)

Melisa Isabel Barolo ¹, María Victoria Castelli ² and Silvia Noelí López ^{2,*}

¹ Farmacognosia, Facultad de Ciencias Bioquímicas y Farmacéuticas, Universidad Nacional de Rosario, Suipacha 531, Rosario S2002LRK, Santa Fe, Argentina; melisabarolo@hotmail.com

² Farmacognosia, Facultad de Ciencias Bioquímicas y Farmacéuticas, Universidad Nacional de Rosario, CONICET, Suipacha 531, Rosario 2002LRK, Santa Fe, Argentina; mcastel@fbioyf.unr.edu.ar

* Correspondence: slopez@fbioyf.unr.edu.ar; Tel.: +54-341-4804592; Fax: +54-341-4804598

Abstract: The endophytic fungal biodiversity of unique plants like *Peperomia argyreia* (Miq.) É. Morren (Piperaceae) has antimicrobial properties and can be employed for infection treatment. Fungal isolates were obtained from appropriately treated plant tissues cultured in solid media, characterized by morphology, and identified by molecular biology using ITS and NL primers. The antimicrobial properties of fungal extracts were analyzed by combining microdilution and bioautographic assays complemented with metabolic profiling by automated thin-layer chromatography and ¹H NMR techniques. Thirty-one filamentous fungi were isolated and characterized by ITS and/or D1/D2 region amplification of rDNA, identified as *Thermothielavioides*, *Trichoderma*, *Cyphellophora*, *Cladosporium*, *Arcopilus*, *Plectosphaerella*; *Chaetomium*, *Sporothrix*, *Alboefibula*, and *Penicillium*. *Thermothielavioides* spp. inhibited *Staphylococcus aureus* ATCC 25923; moreover, *Penicillium westlingii* P4 showed inhibitory activity on *Ascochyta rabiei* AR2. The bioactivity-guided fractionation of the EtOAc extract (MIC = 62.5 µg/mL) of *P. westlingii* P4 allowed the purification of citrinin as the main inhibitory compound (MIC = 62.5 µg/mL). *Peperomia argyreia* harbors a rich and diverse endophytic community able to produce bioactive molecules. Citrinin, with a minor influence of volatile compounds biosynthesized by *P. westlingii* P4, was responsible for the inhibition of *A. rabiei* AR2.

Keywords: endophytic fungi; *Peperomia argyreia*; chemical profiling; antimicrobial activity; Piperaceae



Citation: Barolo, M.I.; Castelli, M.V.; López, S.N. Antimicrobial Activity of Fungal Endophytes Associated with *Peperomia argyreia* (Piperaceae). *Appl. Microbiol.* **2024**, *4*, 753–770. <https://doi.org/10.3390/applmicrobiol4020052>

Academic Editor: Alessandro Vitale

Received: 14 March 2024

Revised: 25 April 2024

Accepted: 26 April 2024

Published: 5 May 2024



Copyright: © 2024 by the authors. Licensee MDPI, Basel, Switzerland. This article is an open access article distributed under the terms and conditions of the Creative Commons Attribution (CC BY) license (<https://creativecommons.org/licenses/by/4.0/>).

1. Introduction

Endophytic fungi are a group of fascinating host-associated fungal communities that colonize the intercellular or intracellular spaces of host tissues, providing beneficial effects to their hosts while gaining advantages in return [1]. As a consequence of the complex interactions established between plant hosts and endophytes, they have evolved to develop a huge capacity for producing unique secondary metabolites that are biosynthesized and secreted as powerful tools for their survival and adaptation to the environment.

The genus *Peperomia* Ruiz and Pav. belongs to the Piperaceae family and is composed predominantly of succulent perennial plants, epiphytes, geophytes, and parasites [2], which grow in a wide variety of shapes and sizes in a pantropical distribution [3,4]. On the American continent, the genus is composed of approximately 1600 species [2]. Several hundreds of specialized bioactive metabolites have been described in *Peperomia* species, including phenylpropanoids, flavonoids, lignans, amides, polyketides, terpenoids, meroterpenoids, and chromenes [5].

The species *Peperomia argyreia* (Miq.) É. Morren (synonyms: *Peperomia arifolia* var. *argyreia* Miq., *Peperomia sandersii* C. DC.), popularly known as Peperomia watermelon due to the similarity of its leaves with the watermelon fruit, is usually employed to ornament domestic environments. According to the Scopus database (www.scopus.org; accessed on 14 December 2023), there is one report related to the chemical composition of this

species, describing the presence of phenols, flavonoids, quinones, alkaloids, terpenoids, and saponins. In addition, the inhibitory activity of *P. argyreia* extracts against the alpha-glucosidase enzyme ($IC_{50} = 48.70 \mu\text{g/mL}$) was evaluated [6]. Moreover, no studies have been reported on the endophyte fungal population of this species.

Agriculture is one of the most important sources of economic income in Argentina. The cultivation of legumes (chickpeas, lentils, peas) represents a growing percentage of production together with traditional crops such as soybeans, wheat, corn, or sunflower. According to a recent report, USD 6 out of 10 that Argentina receives as an export belongs to the bioindustrial agro complex [7]. Searching for natural alternatives for phytopathogenic agent control has arisen in the last decades; microorganisms, extracts, or even purified compounds are eligible for biotechnological development nowadays [8]. Previously, we described the fungal endophytic population associated with *Peperomia obtusifolia*, with *Diaporthe* spp. and *Fusarium oxysporum* as the most frequently isolated fungi. *Diaporthe* spp. showed promising inhibitory activity against the chickpea phytopathogenic fungus *Ascochyta rabiei*, responsible for the Ascochyta blight [9,10]. As a continuation of our research project devoted to isolating, characterizing, and determining the metabolic and bioactivity profiling of fungal endophytes related to plants with strategic importance, the current research reports the characterization of the endophytic fungal population associated with *P. argyreia* whole plant, their metabolic profiling and antimicrobial properties against a panel of human pathogenic bacteria (*Staphylococcus aureus*, *Staphylococcus epidermidis*, *Escherichia coli*), human opportunistic and pathogenic yeasts (*Candida albicans*, *Candida tropicalis*, *Saccharomyces cerevisiae*, *Cryptococcus neoformans*), and plant pathogenic fungi (*Ascochyta rabiei*, *Fusarium solani*, *Fusarium oxysporum*). Moreover, we describe the bio-guided purification process to isolate and characterize citrinin, the compound responsible for the inhibition of *A. rabiei* in *Penicillium westlingii* P4 extract.

2. Materials and Methods

Plant material: Healthy *Peperomia argyreia* (Miq.) É. Morren (Piperaceae) plants were purchased from the local market (Rosario, Santa Fe) in June 2015 for the isolation of fungal endophytes. One specimen was herborized and deposited in the herbarium collection of the Faculty of Agricultural Sciences, UNR (admission number Barolo 11014) [11].

Isolation of fungal endophytes: Leaves, petioles, stems, and roots of *P. argyreia* were collected and processed within 2 h after collection. Plant surface sterilization and isolation of fungal endophytes were carried out following previously described procedures [12]. Surface-sterilized samples were aseptically crumbled into small fragments ($0.5\text{--}1 \text{ cm}^2$) and evenly placed on 60 mm Petri dishes (one fragment per dish) containing potato dextrose agar (PDA), Sabouraud glucose agar (SGA), Czapek agar (CA), and water agar (WA). A total of 63 fragments (42 from leaves, 21 from petioles, 15 from roots, 18 from flowers, and 3 fragments from each tissue crushed under liquid nitrogen) were processed. Petri dishes were incubated for up to 40 days at $28 \text{ }^\circ\text{C}$ in darkness. An aliquot of the sterile water used for the last washing step was concentrated 10 times by centrifugation, and 0.1 mL was spotted on PDA dishes and incubated under the same conditions as a control of the disinfection process. Cultures were evaluated periodically to monitor the growth of endophytic fungi. For each fungal development, sub-cultures in PDA were carried out to obtain pure colonies. Culture purity was assessed after incubation at $28 \text{ }^\circ\text{C}$ for 7 days in darkness by colony morphological evaluation. Pure cultures were maintained on PDA for further investigation or stored in 5% (*v/v*) glucose and 10% (*v/v*) glycerol at $-80 \text{ }^\circ\text{C}$ and in sterile water at room temperature for long-term storage.

Fungal identification: The DNA segments comprising the ITS1 and ITS2 regions of ribosomal DNA were amplified with ITS1 (5'-TCCGTAGGTGAACCTGCGG-3') and ITS4 (5'-TCCTCCGCTTATTGATATGC-3') primers in a 96-well thermocycler (Applied Biosystems®, Waltham, MA, USA). In cases where it was not possible to use the ITS1 and ITS4 primers [13], the primers NL1 (5'-GCATATCAATAAGCGGAGGAAAAG-3') and NL4 (5'-GGTCTGTGTTTCAAGACGG-3') that amplify the variable domains D1 and D2 of

the 28S rRNA were used [14]. For P4 isolate, a region of the β -tubulin gene was also amplified with the primers Bt2a (5'-GGTAACCAAATCGGTGCTGCTTTC-3') and Bt2b (5'-ACCCTCAGTGTAGTGACCCTTGGC-3') [15] under the same reaction conditions used for primers ITS1-ITS4 and NL1-NL4. The reaction mix composition and the parameters employed were from Scholtz et al. 2016 with minimal modifications [16].

The reaction products were analyzed on a 2% agarose gel (Invitrogen[®], Waltham, MA, USA) (electrophoretic run at 140 V, 20 min) developed with Gel Green[®] (Biotium, Fremont, CA, USA) and observed on an UltraBright Transilluminator (Maestrogen, Hsinchu, Taiwan) at 470 nm. Fragments were purified using the AxyPrep PCR Clean-up kit (Axygen[®]) following the manufacturer's instructions. PCR products were sequenced (Macrogen, Seoul, Republic of Korea) using the primers ITS1, ITS4, NL1, and Bt2a as appropriate. The sequences were edited (Chromas 2.6.5, www.technelysium.com.au (Free download, accessed on 24 July 2018) and compared with the GenBank database using BLAST (<https://blast.ncbi.nlm.nih.gov/Blast.cgi> (accessed on 15 January 2024)). Sequence similarities were considered greater than or equal to 97% for identification at the species level, with coverage greater than or equal to 80% [17] and sequence similarities greater than or equal to 90% for identification at the genus level [18].

Extract preparation of endophytic fungi: The fungi were cultivated for 21 days at 28 °C in the dark in Petri dishes of 6 cm in diameter with PDA. Six plates were used for each fungus, and a culture medium blank (six plates) was made. After that time, the culture medium was divided into cubes of approximately 5 mm and macerated with EtOAc (150 mL total/fungus), performing 3 consecutive cycles of 24 h with a sonication period of 15 min each. The organic phase was dried with anhydrous Na₂SO₄, then filtered, and the solvent was removed in a rotary evaporator (Heidolph, Germany) at 30 °C. The crude extracts were stored at −20 °C until use. The resulting organic phase was then dried using anhydrous Na₂SO₄, filtered, and the solvent was removed using a rotary evaporator at 30 °C. Finally, the crude extracts were stored at −20 °C until further use.

Nuclear Magnetic Resonance: The ¹H NMR spectra of the extracts were performed in a Bruker[®] AV-300 (Billerica, MA, USA) operating at a frequency of 300.13 MHz at 25 °C. Spectra of ¹H NMR were made with CDCl₃ and consisted of 64 scans. The concentration of the extracts was from 6 to 12 mg/mL. The data were processed using the software Bionumerics v7.6 (Trial version Applied Maths, Biomerieux, Belgium).

Automated thin-layer chromatography: The extracts were solubilized in EtOAc at a concentration of 10 mg/mL. Then, 10 μ L was applied on TLC quality aluminum sheets (Silica gel 60F254, 1.05554.0001 Merck[®], Rahway, NJ, USA) in 4 mm bands, and the plates were developed automatically for 7 cm (ATS 4 and ACD 2, CAMAG[®], Muttenz, Switzerland), using 3 different mobile phases: Hex: EtOAc (7:3), DCM: EtOAc:MeOH (9:0.5:1), and EtOAc:MeOH:H₂O (7.7:1.3:1). UV 254 nm, UV 366 nm, light white and 10% H₂SO₄ in MeOH [19]. Data were digitized (TLC Visualizer, CAMAG[®]) and processed with Vision-CATS v3.1 software (CAMAG, Muttenz, Switzerland).

Bioautography: Extracts were directly deposited as spots or bands onto silica gel plates (Silica gel 60 F254, 1.05554.0001 Merck[®]). TLC plates were developed in appropriate solvent systems when needed and allowed to air dry until complete solvent evaporation, followed by 20 min UV light sterilization. Bacterial strains evaluated were *Staphylococcus aureus* ATCC 25923 and *Escherichia coli* ATCC 25922; yeast: *Candida albicans* ATCC 10231, *Candida tropicalis* CCC 131-1997, *Cryptococcus neoformans* ATCC 32264, *Rhodotorula rubra* CCC 131-2009 and *Saccharomyces cerevisiae* ATCC 9763 and the filamentous fungi *Ascochyta rabiei* (isolate AR2) and *Verticillium* sp. Bacterial strains were cultured in Mueller–Hinton (MHA) culture medium, the yeasts in SGA, meanwhile, filamentous fungal strains were cultured in PDA. A soft culture (0.75% agar) of the corresponding culture medium (MHA, SGA, or PDA) was melted, and once warmed, a fresh suspension of fungal spores, yeast cells, or bacterial cells was added to give a desired final concentration of 1×10^5 conidia or yeasts/mL or 1×10^6 bacteria/mL and was distributed over the TLC plate (0.1 mL/cm²). After solidification, plates were incubated at 24 °C (*A. rabiei*) or at 28 °C (yeasts and

Verticillium sp.) for 48 h or at 37 °C (bacteria) for 24 h in a humid sterile atmosphere. Yellowish halos against a violet background of the microbial growth that were visualized after spraying TLC plates with a sterile 1 mg/mL MTT solution (methylthiazolyldiphenyl-tetrazolium bromide, Merck, Darmstadt, Germany) were attributable to microbial growth inhibition [20].

MALDI ToF MS proteomic analysis: Mycelial portions of fungal strains cultured in SGA were placed in centrifuge tubes containing 300 µL water and vortexed vigorously for 1 min; after that, 900 µL was added and again vortexed vigorously 1 min before centrifugation (16,000 rpm for 2 min). The supernatant was discarded, and the pellets were dried.

Pellets were resuspended in 50 µL formic acid (70%) and vortexed 1 min. Afterward, 50 µL acetonitrile (100%) was added to the mixture and vortexed for 1 min before centrifugation (13,000 rpm for 2 min). The supernatant (1 µL) was directly spotted onto an MSP96 steel target plate (Bruker Daltonics GmbH, Bremen, Germany) and allowed to air-dry for 15 min. A 1 µL droplet of the α-cyano- 4-hydroxycinnamic acid (CHCA) matrix solution previously prepared by dissolving 10 mg matrix powder (Bruker Daltonics GmbH) in 100 mL trifluoroacetic acid (TFA 3%) + 400 mL deionized water + 500 mL acetonitrile was applied over the dried sample and air-dried for 15 min. Analyses were performed on a MicroFlex LT MALDI-ToF mass spectrometer (Bruker Daltonics GmbH) with a nitrogen laser (337 nm) with 20–65% intensity. A protein extract of *Escherichia coli* (Bruker Daltonics GmbH) was used for external calibration of the equipment. Each spectrum was obtained after an average of 40 laser shots at six different spot positions at 60 Hz, and signals were automatically collected with the AutoXecute tool of the FlexControl acquisition software 3.3 (Bruker Daltonics GmbH), mass range = 2000–20,000 *m/z* at linear mode. Spectra were used in further analyses when the peaks showed a resolution higher than 200. Data were exported as txt files, and the comparison of the spectral profiles and data processing was carried out by similarity analysis using Bionumerics software 7.6 (Trial version Applied Maths, Biomerieux, Belgium).

Evaluation of the interaction of *P. westlingii* P4 with *A. rabiei*: First, 7 mm diameter discs were cut from 7-day-old colonies and seeded in Petri dishes 9 cm in diameter with PDA medium; they were incubated for 21 days at 25 °C in the dark, in triplicate and repeated twice. The interaction was evaluated by taking photographs with the TLC Visualizer camera (Camag®) at 7, 14, and 21 days of growth. After that time, 3 extractions were performed (maceration with EtOAc, sonicating 15 min) from the region where *P. westlingii* developed and the region where there was no development of either fungus (only diffusion of metabolites for interaction with *A. rabiei*). All extracts were evaluated by TLC.

Inhibition of the mycelial growth of *A. rabiei*: The antifungal activity of the purified fraction was evaluated following the methodology described by Soyulu et al. (2006) with some modifications [21]. First, 7 mm diameter discs of 7-day-old *A. rabiei* colonies were cut and seeded in the center of Petri dishes of 5 cm in diameter with PDA medium added with the crystallized fraction to a final concentration of two times the MIC (125 µg/mL), and PDA medium was used as a control. In each case, 5 replicates were used and incubated for 21 days at 25 °C in the dark. The experiments were conducted twice. The mean radial growth of the mycelium was determined by measuring the diameter of the colony in two directions at right angles at 7, 14, and 21 days. The mean growth values were determined and then converted into the percentage of inhibition of mycelial growth relative to the control using the formula:

$$\text{MGI\%} = \frac{d_{\text{control}} - d_{\text{treat}}}{d_{\text{control}}} \times 100 \quad (1)$$

where d_{control} and d_{treat} represent the growth diameter in control and treated Petri dishes, respectively.

Determination of volatile compounds in the inhibition of *A. rabiei*: The effects of the endophytic volatile metabolites toward mycelial growth of *A. rabiei* were evaluated

following the methodology described by Fleitas Centurión and Grabowski Ocampos (2014) with some modifications [22]. Disks of 7 mm diameter were cut from *A. rabiei* colonies of 7 d growth and planted in the center of Petri dishes of 5 cm diameter with PDA medium, proceeding in the same way with the endophytic *P. westlingii* (with 1 d of growth, since it presents a rapid development of conidia and to avoid the dispersion of them). After that, the plates were paired, leaving the antagonist at the base and the phytopathogen at the top, and then sealed with parafilm. As a control, plates were used with *A. rabiei* facing a base without an antagonist (only with PDA medium). In each case, 5 replicates were used and incubated for 21 days at 25 °C in the dark. The experiments were conducted twice. The mean radial growth of the mycelium was determined by measuring the diameter of the colony in two directions at right angles at 7, 14, and 21 days. The mean growth values were determined and then converted into percentage of inhibition of mycelial growth in relation to the control by using Formula (1).

Extract preparation, fractionation of *P. westlingii* P4, purification and identification of citrinin: Punctual seedings of *P. westlingii* P4 one-week-old PDA cultures were performed in the center of 90 Petri dishes of 5 cm diameter containing PDA. The plates were incubated for 21 days at 28 °C in the dark. After that, the culture medium was fragmented and macerated with 900 mL EtOAc (3 × 24 h) with sonication periods of 15 min. The resulting extract was dried over Na₂SO₄ anhydrous, and the solvent was removed under rotary evaporation at 30 °C. The resulting organic extract (735.7 mg) was submitted to a chromatographic separation on Silica gel 60 Merck® (0.040–0.063 mm) employing a gradient of solvents starting with 100% dichloromethane (DCM) and increasing the polarity by adding EtOAc 5% in steps, ending with EtOAc:MeOH 50:50 and 100% MeOH. Nine fractions (Fr 1–9) were obtained. Fractions 2 (88.0 mg) and 3 (47.0 mg) were pooled and submitted to the crystallization process. The crystalline product (2–3Cr, 50.9 mg) was analyzed by HRMS-MS (LCMS MICRO QToF II, Bruker®, Billerica, MA, USA) and NMR (¹H; ¹³C; H-H COSY; HSQC; HMBC) and was identified as citrinin (see Supplementary Material Figures S1–S7). Optical rotation was determined on a JASCO DIP-1000 polarimeter (Jasco, Japan) with a sodium lamp (589 nm, line D) and an optical path cell of 10 mm.

Minimal Inhibitory Concentration (MIC) on *A. rabiei*: Broth micro-dilution tests were performed following the European Committee on Antimicrobial Susceptibility Testing document (EUCAST) with minor modifications (https://www.eucast.org/eucast_news/news_singleview?tx_ttnews%255Btt_news%255D=481&cHash=8c2e4a8022c212c27ad80e1f24a475e7, accessed on 7 April 2024). The inoculum was used at a final concentration of 1 × 10⁵ conidia/mL. Chlorothalonil was included as a positive control. Concentrations of each sample tested ranged from 800 to 12.5 µg/mL. The MIC was defined as the concentration that produced the complete visual inhibition of fungal growth after 72 h incubation at 24 °C. Doubtful microplate wells were observed under a Leica DM500 light microscope (Leica Microsystems, Wetzlar, Germany) at 40×.

3. Results

3.1. Isolation and Molecular Identification of *P. argyrea* Fungal Endophytes

Thirty-one septate filamentous fungi were isolated from *P. argyrea* tissues and analyzed according to their macro and micromorphology. After 7–10 days of culture on PDA plates at 25–28 °C, 26 strains showed hyaline mycelia; meanwhile, 5 strains appeared as dark septate fungi. Table S1 summarizes the macro-morphological aspects observed (development, appearance), melanin production, and micro-morphological aspects with emphasis on the evidence of asexual reproduction.

The 31 filamentous fungi were identified by amplification, sequencing, and comparison with databases of conserved regions of ribosomal DNA. A region of the β-tubulin gene was also used in the case of P4 isolate (Table 1).

Table 1. Molecular identification of fungal endophytes isolated from *P. argyreia* tissues.

Strain	Isolate ID (GenBank Accession)	GenBank Sequence with Major % of Identity (GenBank Accession)	Match Identity (%)	Query Cover (%)	Primers
P1	<i>Arcopilus</i> sp. (MH165192.1)	<i>Arcopilus globulus</i> (NG_070473.1)	95	100	NL1-NL4
P2	<i>Sporothrix stylites</i> (MH165193.1)	<i>Sporothrix stylites</i> (MH874594.1)	98	100	NL1-NL4
P3	<i>Cladosporium devikae</i> (MH165229.1)	<i>Cladosporium devikae</i> (MZ303808.1)	100	100	ITS1-ITS4
P4	<i>Penicillium</i> sp.	<i>P. miczynskii</i> (NR_077156.1) <i>P. aurantiacobrunneum</i> (NR_121509.1) CBS 126228, <i>P. quebencense</i> (NR_121507.1) CBS 101623, <i>P. ubiquitousum</i> (KX011020.1), <i>P. neomiczynskii</i> (KP714288.1), <i>P. cairnsense</i> (NR_121508.1) CBS 124325, <i>P. westlingii</i> (JN617668.1) CBS 124313, <i>P. decatureense</i> (HM469399.1)	91	97	ITS1-ITS4
	<i>Penicillium westlingii</i> (MH165230.1)	<i>Penicillium westlingii</i> (JN606717.1) CBS 127008	99	90	Bt2a-Bt2b
P5	<i>Chaetomium cupreum</i> (MH165194.1)	<i>Chaetomium cupreum</i> (KJ439108.1)	99	99	NL1-NL4
P6	<i>Trichoderma koningiopsis</i> (MH165231.1)	<i>Trichoderma koningiopsis</i> (NR_131281.1)	100	100	ITS1-ITS4
P7	<i>Trichoderma hamatum</i> (MH165232.1)	<i>Trichoderma hamatum</i> (KT827285.1)	100	99	ITS1-ITS4
P8	<i>Trichoderma koningiopsis</i> (MH165233.1)	<i>Trichoderma koningiopsis</i> (NR_131281.1)	100	100	ITS1-ITS4
P9	<i>Thermothielavioides</i> sp. (MH165195.1)	<i>Thermothielavioides maryleae</i> (OR731504.1)	92	93	NL1-NL4
P10	<i>Thermothielavioides maryleae</i> (MH165196.1)	<i>Thermothielavioides maryleae</i> (OR731504.1)	100	98	NL1-NL4
P11	<i>Thermothielavioides terrestris</i> (MH165197.1)	<i>Thermothielavioides terrestris</i> (OR731504.1)	100	98	NL1-NL4
P12	<i>Thermothielavioides maryleae</i> (MH165198.1)	<i>Thermothielavioides maryleae</i> (OR731504.1)	98	100	NL1-NL4
P13	<i>Thermothielavioides</i> sp. (MH165199.1)	<i>Thermothielavioides terrestris</i> (MK926837.1)	91	99	NL1-NL4
P14	<i>Thermothielavioides maryleae</i> (MH165200.1)	<i>Thermothielavioides maryleae</i> (OR731504.1)	97	100	NL1-NL4
P15	<i>Thermothielavioides maryleae</i> (MH165201.1)	<i>Thermothielavioides maryleae</i> (OR731504.1)	98	100	NL1-NL4

Table 1. Cont.

Strain	Isolate ID (GenBank Accession)	GenBank Sequence with Major % of Identity (GenBank Accession)	Match Identity (%)	Query Cover (%)	Primers
P16	<i>Thermothielavioides</i> sp. (MH165202.1)	<i>Thermothielavioides maryleeae</i> (OR731504.1)	86	99	NL1-NL4
P17	<i>Thermothielavioides</i> sp. (MH165203.1)	<i>Thermothielavioides terrestris</i> (MK926837.1)	93	99	NL1-NL4
P18	<i>Thermothielavioides maryleeae</i> (MH165204.1)	<i>Thermothielavioides maryleeae</i> (OR731504.1)	98	100	NL1-NL4
P19	<i>Plectosphaerella cucumerina</i> (MH165234.1)	<i>Plectosphaerella cucumerina</i> (LR026809.1)	100	100	ITS1-ITS4
P20	<i>Cyphellophora</i> sp. (MH165235.1)	<i>Cyphellophora goniomatis</i> (NR_166332.1)	91	84	ITS1-ITS4
P21	<i>Thermothielavioides maryleeae</i> (MH165205.1)	<i>Thermothielavioides maryleeae</i> (OR731504.1)	98	100	NL1-NL4
P22	<i>Thermothielavioides maryleeae</i> (MH165206.1)	<i>Thermothielavioides maryleeae</i> (OR731504.1)	98	100	NL1-NL4
P23	<i>Thermothielavioides maryleeae</i> (MH165207.1)	<i>Thermothielavioides maryleeae</i> (OR731504.1)	97	100	NL1-NL4
P24	<i>Thermothielavioides maryleeae</i> (MH165208.1)	<i>Thermothielavioides maryleeae</i> (OR731504.1)	98	100	NL1-NL4
P25	<i>Thermothielavioides</i> sp. (MH165209.1)	<i>Thermothielavioides maryleeae</i> (OR731504.1)	95	100	NL1-NL4
P26	<i>Thermothielavioides</i> sp. (MH165210.1)	<i>Thermothielavioides maryleeae</i> (OR731504.1)	95	99	NL1-NL4
P27	<i>Alboefibula</i> sp. (MH165236.1)	<i>Alboefibula bambusicola</i> (NR_175177.1)	93	100	ITS1-ITS4
P28	<i>Thermothielavioides</i> sp. (MH165211.1)	<i>Thermothielavioides maryleeae</i> (OR731504.1)	92	99	NL1-NL4
P29	<i>Thermothielavioides maryleeae</i> (MH165212.1)	<i>Thermothielavioides maryleeae</i> (OR731504.1)	98	100	NL1-NL4
P30	<i>Thermothielavioides maryleeae</i> (MH165213.1)	<i>Thermothielavioides maryleeae</i> (OR731504.1)	98	100	NL1-NL4
P31	<i>Cyphellophora</i> sp. (MH165237.1)	<i>Cyphellophora goniomatis</i> (NR_166332.1)	91	81	ITS1-ITS4

Sequence similarities greater than or equal to 97% with coverage greater than or equal to 80% were considered for species identification [17]. Meanwhile, sequence similarities greater than or equal to 90% were considered for identification at the genus level when the ITS region was used [18]. The same criterion was taken for the D1 and D2 regions of the 28S rRNA and β -tubulin gene. Figure 1 shows the distribution in genera of the fungal endophytes from *P. argyreia*.

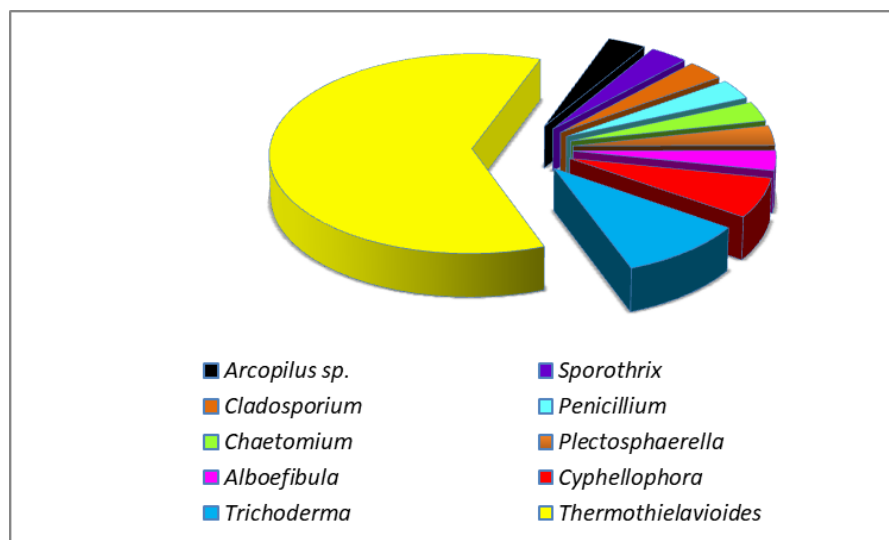


Figure 1. Distribution of the genera of the fungal endophytes isolated from *Peperomia argyreia* (Piperaceae).

A total of 9 fungi were sequenced using the ITS1-ITS4 primer (P3, P4, P6–P8, P19, P20, P27, P31), while the remaining 22 fungi (P1, P2, P5, P9–P18, P21–P26, P28–P30) were analysed by primers NL1 and NL4 due to the better results obtained.

The comparison of the amplified sequences with the Basic Local Alignment Search Tool (BLAST) (<https://blast.ncbi.nlm.nih.gov/Blast.cgi> (accessed on 15 January 2024) limiting searches to sequences from type material, allowed to identify 18 isolates to *Thermothielavioides* genus (P9–P18, P21–P26, P28–P30), 3 isolates to *Trichoderma* (P6–P8), 2 isolates to *Cyphellophora* (P20, P31), and individual representatives to *Arcopilus* (P1), *Sporothrix* (P2), *Cladosporium* (P3), *Penicillium* (P4), *Chaetomium* (P5), *Plectosphaerella* (P19), and *Alboefibula* (P27) genera (Table 1).

In regard to *Thermothielavioides*, 61% of the isolates were identified as *T. marileae* (P10, P12, P15, P18, P21–P24, P29, and P30), followed by *T. terrestris* (P11, 5%); meanwhile, the isolates P13, P17, P25, P26, and P28 remained as *Thermothielavioides* sp. due to a % match identity of less than 97% when compared with sequences from type material.

The isolates P6–P8 were identified as *Trichoderma*, being P6 and P8 *T. koningiopsis* and P7 *T. hamatum*. The isolates P20 and P31 were identified as *Cyphellophora* sp., P1 as *Arcopilus* sp., and P27 as *Alboefibula* sp. Moreover, the isolates P2, P3, P5, and P19 were identified as species being *Sporothrix stylites*, *Cladosporium devikae*, *Chaetomium cupreum*, and *Plectosphaerella cucumerina*, respectively.

The isolate P4 was initially identified as *Penicillium* sp. through ITS4 primer amplification; after that, the region of the β -tubulin gene was amplified to identify it as the species *P. westlingii* (P4).

3.2. MALDI ToF MS of the Fungal Isolates

MALDI ToF MS was applied as a complementary tool to characterize fungal isolates, particularly those identified as *Thermothielavioides* spp. Mycelia obtained under standardized conditions were treated to obtain spectral profiles of fungal ribosomal proteins. Despite the robustness demonstrated by this technique for the identification of clinically important

bacteria and fungi, its application to environmental samples remains challenging due to the lack of commercial and open-access databases, including environmental fungi. The obtained spectra were compared in a similarity matrix (Figure 2) with the identification obtained by molecular biology (Table 1). *Arcopilus* sp. (P1) showed moderate similarity with *Chaetomium cupreum* (P5); *Cyphellophora* spp. P20 and P31 spectra were grouped with high similarity, whilst the major pattern of similarity was observed for *Thermothielavioides* spp. spectra, with high similarity match amongst P23 with P29, P10, P13, P17 and P25 spectra, and between P11 with P18, P26, P14, and P12. Interestingly, the 3 isolates identified as *Trichoderma* (P6–P8) did not form a cluster; instead, they were dispersed from each other in the similarity matrix.

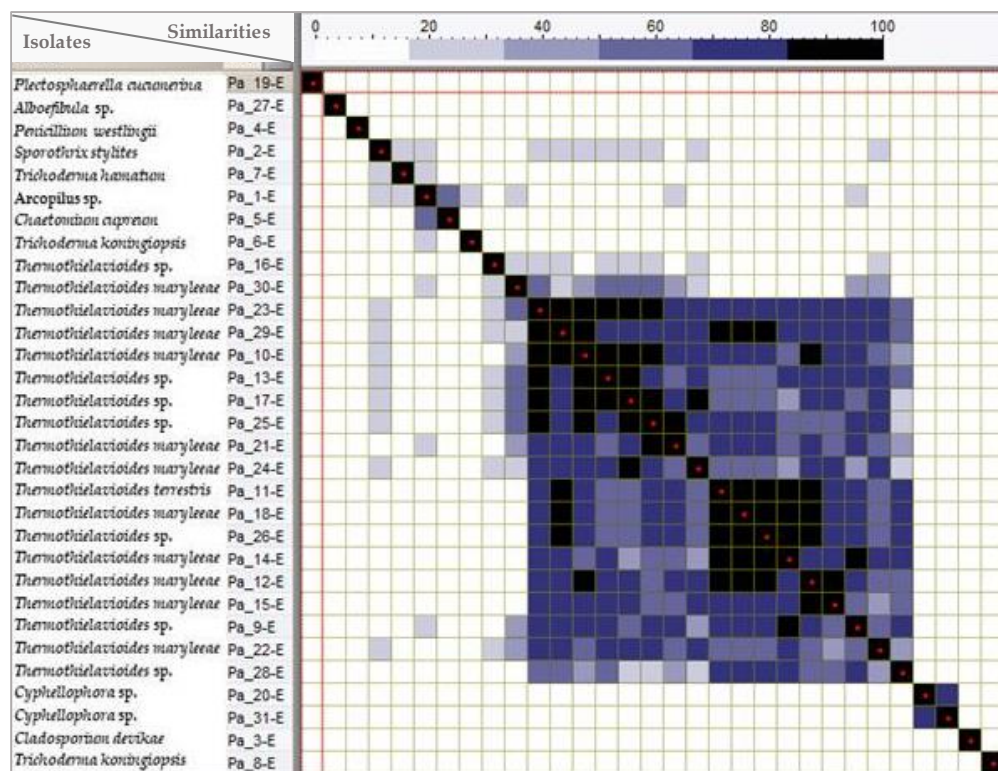


Figure 2. Similarity matrix of MALDI spectra from the fungal endophytes isolated from *P. argyreia*. To the left of each isolate code is the identification obtained by the molecular biology tool. Similarity scale (white to black 0–100%): white 0–18%; light gray 18–32%; gray 32–50%; dark gray 50–66%; blue 66–83%; black 83–100%.

3.3. Nuclear Magnetic Resonance

The multivariate analysis of the ^1H NMR spectra obtained from the extracts of the endophytic fungi of *P. argyreia* showed a clear differentiation of the endophytic *P. westlingii* P4 and a grouping of *C. cupreum* P5 and *Arcopilus* sp. P1. The three principal components explained 71.3% of the total variability of the original data (Figure 3). This observation complements the results obtained by MALDI-ToF MS, where P1, identified by sequencing as *Arcopilus* sp., grouped with *C. cupreum* P5 with a high percentage of similarity (91.72%).

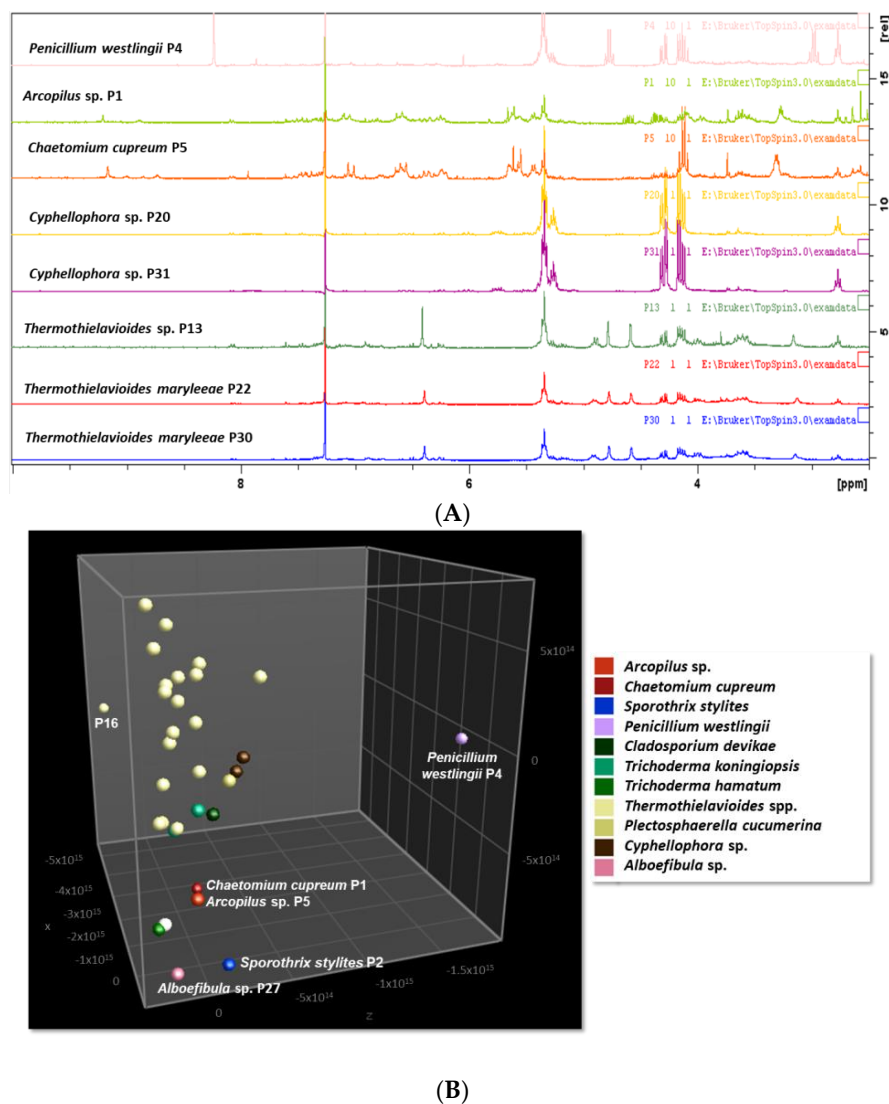


Figure 3. (A) ¹H NMR (300 MHz, CDCl₃) spectra of selected extracts of the endophytic fungi P4, P1, P5, P20, P31, P13, P22, and P30 isolated from *P. argyrea*. (B) PCA of the ¹H NMR spectra of the extracts of the 31 endophytic fungi isolated from *P. argyrea*.

3.4. Antimicrobial Activity

Spots containing 10 to 100 µg of EtOAc extracts from the fungal endophytes cultured in PDA were evaluated by spot agar overlay bioautography against a panel composed of the bacteria *Staphylococcus aureus* ATCC 25923 and *Escherichia coli* ATCC 25922, the yeasts *Candida albicans* ATCC 10231, *Candida tropicalis* CCC 131-1997, *Cryptococcus neoformans* ATCC 32264, *Rhodotorula rubra* CCC 131-2009, and *Saccharomyces cerevisiae* ATCC 9763, and crop phytopathogenic filamentous fungi *Ascochyta rabiei* (isolate AR2) and *Verticillium* sp. Twenty-two extracts (71.0%) showed antibacterial properties against *S. aureus*; two extracts (*Arcopilus* sp. P1 and *Chaetomium cupreum* P5) inhibited *E. coli*, whilst *P. westlingii* P4 extract showed activity against *A. rabiei*. The extracts from P3, P6–P8, P16, P19, P20, P27, and P31 were inactive against all the microorganisms tested. Relevant results are summarised in Table 2. Extracts from *P. westlingii* P4 and *C. cupreum* P5 showed better results (inhibition at 25 µg/spot in two microorganisms, Table 2) and were selected for further analysis. After several repetitions, the inhibitory activity of the *C. cupreum* P5 extract was not reproducible. Consequently, the study was centered on the *P. westlingii* P4 isolate, focusing on its antifungal activity observed on *A. rabiei*.

Table 2. Antimicrobial activity of selected fungal endophyte extracts isolated from *P. argyreia* performed by spot agar overlay bioautography. The lowest load ($\mu\text{g}/\text{spot}$) at which the inhibition was observed is expressed.

	Microorganism Tested		
	<i>E. coli</i> ATCC 25922	<i>S. aureus</i> ATCC 25923	<i>A. rabiei</i> AR2
P1— <i>Arcopilus</i> sp.	100	100	—*
P2— <i>Sporothrix stylites</i>	-	100	-
P4— <i>Penicillium westlingii</i>	-	25	25
P5— <i>Chaetomium cupreum</i>	25	25	-
P9— <i>Thermothielavioides</i> sp.	-	25	-
P10— <i>Thermothielavioides maryleeae</i>	-	50	-
P11— <i>Thermothielavioides terrestris</i>	-	100	-
P12— <i>Thermothielavioides maryleeae</i>	-	25	-
P13— <i>Thermothielavioides</i> sp.	-	25	-
P14— <i>Thermothielavioides maryleeae</i>	-	25	-
P15— <i>Thermothielavioides maryleeae</i>	-	100	-
P17— <i>Thermothielavioides</i> sp.	-	100	-
P18— <i>Thermothielavioides maryleeae</i>	-	100	-
P21— <i>Thermothielavioides maryleeae</i>	-	100	-
P22— <i>Thermothielavioides maryleeae</i>	-	25	-
P23— <i>Thermothielavioides maryleeae</i>	-	25	-
P24— <i>Thermothielavioides maryleeae</i>	-	100	-
P25— <i>Thermothielavioides</i> sp.	-	25	-
P26— <i>Thermothielavioides</i> sp.	-	100	-
P28— <i>Thermothielavioides</i> sp.	-	100	-
P29— <i>Thermothielavioides maryleeae</i>	-	25	-
P30— <i>Thermothielavioides maryleeae</i>	-	100	-
Chlorotalonyl	-	-	0.5
Vancomycin	0.3	0.3	-

Note: *—: inactive at 100 $\mu\text{g}/\text{spot}$.

3.5. Inhibitory Effect of *P. westlingii* P4 on *A. rabiei*

3.5.1. Chemical Profile and Antifungal Activity

The EtOAc extract obtained from 90 plates in APD was fractionated by a silica gel column to obtain 10 fractions. Fractions 2 and 3 were compared using TLC and combined, and the product was recrystallized. The 2-3Cr product was active against *A. rabiei* with a MIC of 62.5 $\mu\text{g}/\text{mL}$ (MIC of chlorothalonil = 1 $\mu\text{g}/\text{mL}$), being mainly responsible for the activity detected in the initial screening by bioautography (Figure S1). The purity of the fraction was analyzed by TLC and ^1H NMR and was considered acceptable for further structural elucidation experiments.

The analysis of HRMS-MS in (+) mode showed an ion of $m/z = 251.0890$, corresponding to the adduct $[\text{M} + \text{H}]^+$ and an ion of $m/z = 273.0721$, corresponding to the adduct $[\text{M} + \text{Na}]^+$ of citrinin, a mycotoxin isolated for the first time from *Penicillium citrinum* [23]. The HRMS in (-) mode showed an $m/z = 249.0752$, which corresponds to the molecular formula $\text{C}_{13}\text{H}_{14}\text{O}_5$, using a collision energy of 10 eV with a base peak of $m/z = 205.0854$. The results of the NMR experiments and their comparison with the literature [24] allowed the

assignment of the 2-3Cr fraction to the known compound citrinin. Data are available in Supplementary Material (Figures S2–S7).

Citrinin is produced by several *Penicillium* species [25], *Aspergillus* [26], and *Monascus* [27–29]. Its chemical structure was proposed for the first time by Brown et al. in 1948 [30]. The molecule has 2 stereocenters, and the absolute configuration was determined by Hill and Gardella in 1964 [31]. The optical rotation determined for citrinin was coincident with the literature values ($[\alpha]_D$ at 25.0 °C = -28.3463° , c. 0.6597 in absolute ethanol) [32].

3.5.2. Evaluation of the Interaction of *P. westlingii* P4 with *A. rabiei*

The study of the interaction between *P. westlingii* P4 and *A. rabiei* resulted in a clear inhibition of the development of the phytopathogen (Figure 4). Through the evaluation by TLC of the extracts obtained from different regions of the Petri dish, the presence of citrinin could be determined in the culture medium, which would be diffused and thus responsible for the inhibition of *A. rabiei*.

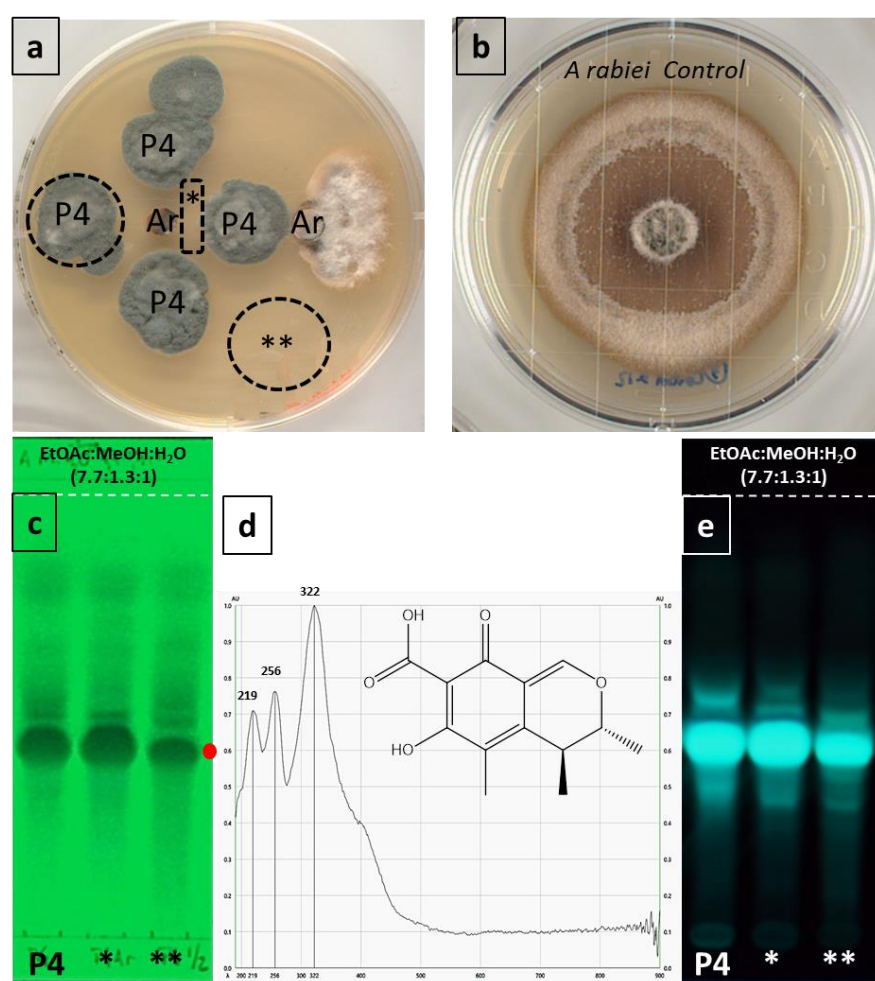


Figure 4. (a) Combined antagonistic effects amongst *P. westlingii* and *A. rabiei* after 21 d in PDA in the dark. (b) Control plate of *A. rabiei* after 21 d in PDA in the dark. (c) UV 254 nm TLC profile comparing EtOAc extracts of P4 colony, a piece of agar between P4 and *A. rabiei* (*), and a section of the PDA medium away from the interactions (**). (d) UV-Vis densitometric spectrum taken from the chromatographic band corresponding to citrinin (red blot). (e) Plate (c) sprayed with H₂SO₄ plus heating observed at 254 nm. Mobile phase: EtOAc:MeOH:H₂O (7.7:1.3:1), extracts: 25 µg/band of 4 mm. Photographs were taken on a TLC Visualizer 2 Camag. Densitometric analysis was performed in a TLC Scanner 4 Camag. (e) a piece of agar between P4 and *A. rabiei* (*); a section of the PDA medium away from the interactions (**).

3.5.3. Determination of Volatile Compounds in the Inhibition of *A. rabiei*

The study of the inhibitory effect of volatile organic compounds biosynthesized by *P. westlingii* P4 showed a low inhibition (20%) of the *A. rabiei* mycelial growth after 7 d. However, the production of pigment, even at 21 d incubation, was completely different from the control, suggesting an affectation in the biosynthesis of melanin.

3.5.4. Inhibition of the Mycelial Growth of *A. rabiei*

The inhibition of radial mycelial growth of *A. rabiei* by adding 125 µg/mL citrinin in comparison to the control showed complete inhibition of the development of *A. rabiei* (Figure 5).

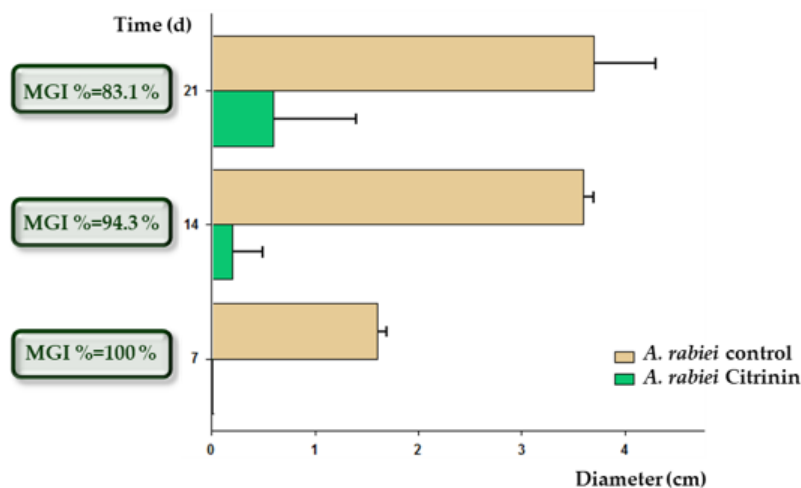


Figure 5. Comparison of the development of *A. rabiei* in PDA (control) versus in PDA plus 125 µg/mL of citrinin at 7, 14, and 21 d of development at 24 ° C, in the dark. MGI% = Mycelial growth index.

4. Discussion

The study of the endophytic community of *P. argyreia* allowed the isolation of thirty-one filamentous fungi. The identification process was carried out through molecular tools, involving the amplification of the ITS region of the rDNA, complemented with MALDI ToF proteomics. These findings were further corroborated with morphological comparisons and metabolic profiling by 1H NMR.

Among the fungal genera identified as endophytes in this plant, *Penicillium*, *Trichoderma*, *Arcopilus*, and *Thermothielavioides* (synonym: *Thielavia*) have been previously documented in association with *Peperomia* spp. [33,34]. However, *Sporothrix*, *Cladosporium*, *Cyphellophora*, *Albofibula*, and *Plestosphaerella* genera are described here for the first time as endophytes in the *Peperomia* genus.

Interestingly, while Basidiomycota are rarely isolated as endophytes [35], the basidiomycete *Albofibula* sp. was isolated from *P. argyreia* tissues, representing the first report of this fungal genus as an endophyte. In contrast to most studies on fungal endophyte isolation and characterization, conidia production was observed in 27 of 31 fungal isolates (87%).

MALDI-ToF proteomic profiling shows differences amongst many unidentified proteins, which reflects a broader proportion of the total genome than the multigenic sequence-based studies [36]. Although this tool shows extremely high reliability in determining clinically relevant bacteria and yeasts since it is based on robust databases, it failed in the identification of the isolates obtained from *P. argyreia*. Consequently, the data obtained from MALDI were used to assist in the interpretation of results obtained through molecular identification, particularly when no specific species assignment was possible. Spectra were compared using a similarity matrix (Figure 3), and isolates were clustered following the molecular identification obtained previously. The 1H NMR profiling of the EtOAc extracts analyzed by multivariate analysis showed organization patterns associated with chemical

components according to the fungal taxa obtained by molecular identification (Figure 3). The grouping demonstrated a correlation with the molecular identification and MALDI ToF analyses. The three main PCs explain 71.3% of the total variability in the original data. As highlighted before, the separation of the extract from *P. westlingii* P4 in the tridimensional chemical space indicates a distinct chemical composition.

The taxa *Thermotielavioides* sp., *Thermotielavioides maryleeae*, and *Thermotielavioides terrestris* were the most frequently encountered fungi in *P. argyreia*. The amplification of these isolates was carried out using NL1-NL4 primers, as attempts with ITS1-ITS4 primers yielded no amplifications. The isolate P16 exhibited a low match identity with the species *T. maryleeae* (OR731504.1) (Table 1). Furthermore, the comparison of the MALDI ToF proteomic analysis in a similarity matrix also showed a low match with the other *Thermotielavioides* spp. isolates, with only 20–30% similarity with *T. maryleeae* P30 (Figure 2). The PCA of ¹H NMR spectra revealed a similar profiling, with P16 extract separated from the other *Thermotielavioides* extracts (grayish dots, Figure 3B).

Twenty-two extracts demonstrated inhibitory activity against at least one of the tested bacteria, yeasts, and/or fungi. *Staphylococcus aureus* was the most sensitive bacteria tested. Considering the numerous approaches to discovering new antibacterial bioactive compounds, the study of less well-known species and genera of microorganisms is one of the most well-established techniques in the field of natural products [37].

Eighteen out of nineteen strains identified as *Thermotielavioides* spp. showed inhibitory activity on *S. aureus* ATCC 25923 in the bioautographic assay, eight of them even at 25 µg/spot (strains 9, 12–14, 22, 23, 25, 29). Our results are in agreement with previous studies, which highlight the selectivity of endophyte fungal metabolites on Gram-positive bacteria, including multidrug-resistant *S. aureus* strains [38]. While the *Thermotielavioides* genus has been studied for thermophilic enzyme production, studies about its bioactivity and secondary metabolite profiling are limited. In 2019, Wang et al. re-evaluated its related genus *Thielavia* by multi-gene phylogenetic analyses (rpb2, tub2, ITS, and LSU); based on the phylogenetic relationships of the species studied, *Thermotielavioides* was considered as a *Thielavia*-like genus [39]. The isolate P16 deserves more studies to determine its identification with higher match identity scoring. The antibacterial activity on *S. aureus* showed by all the isolates identified as *Thermotielavioides* spp. merits additional investigations to characterize the active metabolites.

As stated above, extracts from *P. westlingii* P4 and *C. cupreum* P5 showed better results, displaying inhibition at 25 µg/spot against two microorganisms (Table 2). However, the study was centered on the *P. westlingii* P4 isolate, focusing on its antifungal activity observed against *A. rabiei*. The quantification of the inhibitory effect of *P. westlingii* P4 EtOAc extract on the *A. rabiei* development showed a MIC of 62.5 µg/mL (MIC Chlorothalonil = 1 µg/mL). The bioactivity-guided fractionation of the total extract allowed the characterization of citrinin, which demonstrated a MIC of 62.5 µg/mL, consistent with that of the full extract. This finding was further validated by an agar diffusion assay, wherein no development of *A. rabiei* was observed even after 21 d (Figure 5). If citrinin is the sole antifungal metabolite in the extract, its MIC should be lower than that of the EtOAc extract. Additional information about the type of interaction between *P. westlingii* P4 and *A. rabiei* was obtained by an interaction study, demonstrating that the only fungal metabolite diffusing into the culture medium near *A. rabiei* was citrinin. Moreover, the investigation of the effect of volatile compounds biosynthesized by *P. westlingii* P4 on the development of *A. rabiei* was inconclusive under the experimental conditions assayed despite showing a qualitative impact on the pigmentation of the mycelial phase. The *Penicillium* genus achieved significant recognition and historical importance through the discovery of penicillin, the beta-lactam secondary metabolite, which revolutionized medical approaches to bacterial diseases in the early 20th century [40,41]. Since then, many other metabolites have been identified in the genus with a wide range of applications [41], including alkaloids, polyketides, and steroids [42–44]. These metabolites are related to cytotoxic activities against human tumor cells [42], antioxidant [45], antiviral [46], antibacterial [47],

and antifungal activities [48]. However, the antifungal activity of this organism against *A. rabiei* (strain AR2) has not been previously reported.

Citrinin is known for its toxic properties in the liver, kidney, heart, and gastrointestinal tract in animals [49]; however, there is growing evidence supporting other biological activities of this molecule, such as anticancer [50] and neuroprotective [51]. This is causing a renewed interest in the research of this natural product. Citrinin has also shown activity against some bacteria, including *S. aureus* (ATCC 29737, NCTC 7447), *Bacillus subtilis*, *Bacillus pumilus*, *Bacillus cereus*, *Shigella dysenteriae*, *Shigella sonnei*, *Shigella boydii*, *E. coli* (ROW 7/12), *Salmonella typhimurium*, *Vibrio cholerae*, *Pseudomonas* sp., *Streptococcus pneumoniae*, among others [52,53], and shows antifungal activity against *C. albicans* (IFM 40009), *C. neoformans* (ATCC 90112), *Aspergillus fumigatus*, and *A. niger* [54]. In the bioautographic tests carried out, it was active against *S. aureus* (ATCC 25923) and *C. neoformans* (ATCC 32264) (minimum load evaluated: 50 µg/spot), but unlike that reported in the literature, it did not show activity against *E. coli* (ATCC 25922) and *C. albicans* (ATCC 10231).

Despite its toxic properties preventing the use of citrinin as a therapeutic drug, it could potentially be applied to the cultivation of chickpeas as an *A. rabiei* inhibitor. It is necessary to establish adequate analytical criteria for analyzing traces of citrinin and its by-products in food. Citrinin can be degraded in an acid or alkaline solution or by heating [55], and this instability could be considered beneficial in the context of its application to chickpea cultivation since the processing of the raw material could contribute to its degradation.

5. Conclusions

Our results demonstrate that *P. argyreia* can live symbiotically with a rich and diverse endophytic community, which also serves as a rich source of bioactive molecules, including those able to inhibit bacteria and phytopathogenic fungi. These findings raise the available knowledge on the fungal endophytic population associated with the *Peperomia* genus.

Thermothielavooides spp. was the most abundant genus isolated; the antibacterial activity shown by their extracts on *S. aureus* deserves more investigations focused on the characterization of the chemical basis of the activity, mode of action, etc. Moreover, *E. coli* was only inhibited for *C. cupreum* P5 extract; meanwhile, *P. westlingii* P4 inhibited *A. rabiei* growth. Further bioguided purification process allowed the isolation and characterization of citrinin.

The results of this study suggest that citrinin could be used in the control of *A. rabiei* as an alternative to synthetic fungicides, as its structure could lead to the development of new classes of antifungal compounds. Demonstrating the biological role of each molecule in nature is a challenge. Therefore, the investigation of natural products in microbial communities becomes a more rational approach since microorganisms interact with each other in their natural environments.

Our observations indicate that citrinin presents greater inhibition of the mycelial growth of *A. rabiei* compared to the volatile compounds biosynthesized by *P. westlingii* P4, which primarily leads to a reduction in the pigmentation of the fungus, probably by inhibition of the melanin biosynthesis.

More research is required to confirm the in vivo effect of the total extract of *P. westlingii* P4 and citrinin as chickpea blight inhibitors. Moreover, the probable presence of other active compounds should also be evaluated.

Supplementary Materials: The following supporting information can be downloaded at: <https://www.mdpi.com/article/10.3390/applmicrobiol4020052/s1>, Table S1: Macro and micromorphological characters of the fungal isolates purified from *Peperomia argyreia* in PDA after 10 d cultivation in darkness at 25 °C; Figure S1: Purification scheme of citrinin from the EtOAc of *P. westlingii* P4. Bioassay fractionation with *A. rabiei* AR2; Figure S2: ¹H NMR spectrum of citrinin in CDCl₃, 300 MHz; Figure S3: ¹³C NMR spectrum of citrinin in CDCl₃, 75 MHz; Figure S4: HSQC experiment of citrinin; Figure S5: HMBC experiment of citrinin; Figure S6: HH COSY citrinin in CDCl₃, 300 MHz; Figure S7: HRMS-MS of citrinin in negative mode. The fragmentation of the ion [M-H]⁻ = 249.0752 is observed. Collision energy = 10 eV.

Author Contributions: Conceptualization, M.V.C. and S.N.L.; Methodology, M.I.B. and M.V.C.; Validation, M.I.B. and M.V.C.; Formal analysis, M.I.B., M.V.C. and S.N.L.; Investigation, M.I.B., M.V.C. and S.N.L.; Resources, M.V.C. and S.N.L.; Data curation, M.V.C. and S.N.L.; Writing—original draft, M.I.B. and S.N.L.; Writing—review & editing, M.V.C. and S.N.L.; Visualization, M.V.C. and S.N.L.; Supervision, S.N.L.; Project administration, S.N.L.; Funding acquisition, S.N.L. All authors have read and agreed to the published version of the manuscript.

Funding: This research was funded by Consejo Nacional de Investigaciones Científicas y Técnicas de Argentina (CONICET, PIP 2120), FONCyT (PICT 2021-GRF-TII-00312), Universidad Nacional de Rosario (UNR, Grant PID 80020180300045UR) and Agencia Santaefesina de Ciencia, Tecnología e Innovación (PEICID-2021-161). MIB acknowledges CONICET for the fellowship. MVC and SNL are members of CONICET.

Data Availability Statement: Data are contained within the article and Supplementary Materials.

Acknowledgments: Authors acknowledge the technical support of Susana Amigot and CEMAR—Municipalidad de Rosario, Argentina, for the MALDI ToF analysis. MIB acknowledges CONICET for the fellowship. MVC and SNL are members of CONICET.

Conflicts of Interest: The authors declare no conflicts of interest.

References

1. Alam, B.; Li, J.; Gě, Q.; Khan, M.A.; Gōng, J.; Mehmood, S.; Yuán, Y.; Gōng, W. Endophytic Fungi: From Symbiosis to Secondary Metabolite Communications or Vice Versa? *Front. Plant Sci.* **2021**, *12*, 791033. [CrossRef]
2. Wanke, S.; Jaramillo, A.; Borsch, T.; Samain, M.S.; Quandt, D.; Neinhuis, C. Evolution of Piperales-matK gene and trnK intron sequence data reveal lineage specific resolution contrast. *Mol. Phylogenet. Evol.* **2007**, *42*, 477–497. [CrossRef] [PubMed]
3. Smith, J.F.; Stevens, A.C.; Tepe, E.J.; Davidson, C.L. Placing the origin of two species-rich genera in the late cretaceous with later species divergence in the tertiary: A phylogenetic, biogeographic and molecular dating analysis of *Piper* and *Peperomia* (Piperaceae). *Plant Syst. Evol.* **2008**, *275*, 9–30. [CrossRef]
4. Valarezo, E.; Herrera-García, M.; Astudillo-Dávila, P.; Rosales-Demera, I.; Jaramillo Fierro, X.; Cartuche, L.; Meneses, M.A.; Morocho, V. Study of the Chemical Composition and Biological Activity of the Essential Oil from Congona (*Peperomia inaequalifolia* Ruiz and Pav.). *Plants* **2023**, *12*, 1504. [CrossRef]
5. Valero Gutierrez, Y.; Yamaguchi, L.F.; Moraes, M.M.; Jeffrey, C.S.; Kato, M.J. Natural products from *Peperomia*: Occurrence, biogenesis and bioactivity. *Phytochem. Rev.* **2016**, *15*, 1009–1033. [CrossRef]
6. Saepudin, S.; Susilawati, Y. Alpha-glucosidase inhibitor activities and phytochemicals screening of the *Peperomia* genus cultivated in Indonesia. *Int. J. Appl. Pharm.* **2022**, *14*, 117–122. [CrossRef]
7. Available online: <https://www.bcr.com.ar/es/mercados/investigacion-y-desarrollo/informativo-semanal/noticias-informativo-semanal/el-agro-aporto> (accessed on 27 December 2023).
8. Pandit, M.A.; Kumar, J.; Gulati, S.; Bhandari, N.; Mehta, P.; Katal, R.; Rawat, C.D.; Mishra, V.; Kaur, J. Major biological control strategies for plant pathogens. *Pathogens*. **2022**, *11*, 273. [CrossRef] [PubMed]
9. Bahr, L.; Castelli, M.V.; Barolo, M.I.; Ruiz Mostacero, N.; Tosello, M.E.; López, S.N. Ascochyta blight: Isolation, characterization, and development of a rapid method to detect inhibitors of the chickpea fungal pathogen *Ascochyta rabiei*. *Fungal Biol.* **2016**, *120*, 424–432. [CrossRef] [PubMed]
10. Ruiz Mostacero, N.; Castelli, M.V.; Barolo, M.I.; Amigot, S.L.; Fulgueira, C.L.; López, S.N. Fungal endophytes in *Peperomia obtusifolia* and their potential as inhibitors of chickpea fungal pathogens. *World J. Microbiol. Biotechnol.* **2021**, *37*, 14. [CrossRef]
11. Available online: <https://fcagr.unr.edu.ar/herbario/> (accessed on 27 December 2023).
12. Schulz, B.; Boyle, C.; Draeger, S.; Rommert, A.K.; Krohn, K. Endophytic fungi: A source of novel biologically active secondary metabolites. *Mycol. Res.* **2002**, *106*, 996–1004. [CrossRef]
13. White, T.J.; Bruns, T.; Lee, S.; Taylor, J. Amplification and direct sequencing of fungal ribosomal RNA genes for phylogenetics. In *PCR Protocols: A Guide to Methods and Applications*; Innis, M.A., Gelfand, D.H., Sninsky, J.J., White, T.J., Eds.; Academic Press: San Diego, CA, USA, 1990; pp. 315–322.
14. Villa-Carvajal, M.R.; Coque, J.J.; Álvarez-Rodríguez, M.L.; Uruburu, F.; Belloch, C. Polyphasic identification of yeasts isolated from bark of cork oak during the manufacturing process of cork stoppers. *FEMS Yeast Res.* **2004**, *4*, 745–750. [CrossRef] [PubMed]
15. Glass, N.L.; Donaldson, G.C. Development of primer sets designed for use with the PCR to amplify conserved genes from filamentous ascomycetes. *Appl. Environ. Microbiol.* **1995**, *61*, 1323–1330. [CrossRef] [PubMed]
16. Scholtz, I.; Korsten, L. Profile of *Penicillium* species in the pear supply chain. *Plant Pathol.* **2016**, *65*, 1126–1132. [CrossRef]
17. Raja, H.A.; Miller, A.N.; Pearce, C.J.; Oberlies, N.H. Fungal identification using molecular tools: A primer for the natural products research community. *J. Nat. Prod.* **2017**, *80*, 756–770. [CrossRef]
18. Nilsson, R.H.; Anslan, S.; Bahram, M.; Wurzbacher, C.; Baldrian, P.; Tedersoo, L. Mycobiome diversity: High-throughput sequencing and identification of fungi. *Nat. Rev. Microbiol.* **2019**, *17*, 95–109. [CrossRef] [PubMed]

19. Reich, E.; Schibli, A. *High Performance Thin-Layer Chromatography for the Analysis of Medicinal Plants*; Thieme Medical Publishers Inc.: New York, NY, USA, 2007; p. 237.
20. Barolo, M.I.; Castelli, M.V.; López, S.N. Antimicrobial properties and biotransforming ability of fungal endophytes from *Ficus carica* L. (Moraceae). *Mycology* **2023**, *14*, 108–132. [[CrossRef](#)] [[PubMed](#)]
21. Soyulu, E.M.; Soyulu, S.; Kurt, S. Antimicrobial activities of the essential oils of various plants against tomato late blight disease agent *Phytophthora infestans*. *Mycopathologia* **2006**, *161*, 119–128. [[CrossRef](#)] [[PubMed](#)]
22. Fleitas Centurión, A.; Grabowski Ocampos, C.J. Biological control of the fungi complex that cause leaf spot on sweet corn (*Zea mays* var. *saccharata*) with beneficial bacteria. *Investig. Agrar.* **2014**, *16*, 83–92.
23. Hetherington, A.C.; Raistrick, H. Studies in biochemistry of microorganism XIV. On the production and chemical constitution of a new yellow colouring matter, citrinin, produced from glucose by *Penicillium citrinum* Thom. *Philos. Trans. R. Soc. Lond. Ser. B—Biol. Sci.* **1931**, *220*, 269–295. [[CrossRef](#)]
24. He, Y.; Cox, R.J. The molecular steps of citrinin biosynthesis in fungi. *Chem. Sci.* **2016**, *7*, 2119–2127. [[CrossRef](#)]
25. Ei-Banna, A.A.; Pitt, J.I.; Leistner, L. Production of mycotoxins by *Penicillium* species. *Syst. Appl. Microbiol.* **1987**, *10*, 42–46. [[CrossRef](#)]
26. Kurata, H. Mycotoxins and mycotoxicoses. In *Microbial Toxins in Foods and Feeds*; Pohland, A.E., Dowell, V.R., Richards, J.L., Eds.; Plenum Press: New York, NY, USA, 1990; pp. 249–259.
27. Blanc, P.J.; Loret, M.O.; Goma, G. Production of citrinin by various species of *Monascus*. *Biotechnol. Lett.* **1995**, *17*, 291. [[CrossRef](#)]
28. Blanc, P.J.; Laussac, J.P.; Le, J.B.; Le, B.P.; Loret, M.O.; Pareilleux, A.; Prome, D.; Prome, J.C.; Santerre, A.L.; Goma, G. Characterisation of monascidin A from *Monascus* as citrinin. *Int. J. Food Microbiol.* **1995**, *27*, 201–213. [[CrossRef](#)] [[PubMed](#)]
29. Samsudin, N.I.; Abdullah, N. A preliminary survey on the occurrence of mycotoxigenic fungi and mycotoxins contaminating red rice at consumer level in Selangor, Malaysia. *Mycotoxin Res.* **2013**, *29*, 89–96. [[CrossRef](#)] [[PubMed](#)]
30. Brown, J.; Cartwright, N.; Robertson, A.; Whalley, W.B. Structure of Citrinin. *Nature* **1948**, *162*, 72–73. [[CrossRef](#)] [[PubMed](#)]
31. Hill, R.K.; Gardella, L.A. The Absolute Configuration of Citrinin 1. *JOC* **1964**, *29*, 766–767. [[CrossRef](#)]
32. Krogh, P.; Hasselager, E.; Friis, P. Studies on fungal nephrotoxicity. *APMIS* **1970**, *78*, 401–413. [[CrossRef](#)]
33. Marcon, E.L. Fungos Endofíticos de Piper Peltatum e Peperomia Pellucida: Caracterização Metabólitos Secundários e Atividades Biológicas. Doctoral Thesis, Federal University of Amazonas, Manaus, Brazil, 2013. Available online: <http://tede.ufam.edu.br/handle/tede/4442> (accessed on 22 January 2024).
34. Gutiérrez, V.; Yasmin, L. Molecular Phylogeny and Secondary Metabolism from Peperomia Species. Doctoral Thesis, Instituto de Química, Universidade de Sao Paulo, São Paulo, Brazil, 2015. [[CrossRef](#)]
35. Chlebicki, A. Some endophytes of *Juncus trifidus* from Tatra Mts. in Poland. *Acta Mycol.* **2009**, *44*, 11–17. [[CrossRef](#)]
36. Panda, A.; Ghosh, A.K.; Mirdha, B.R.; Xess, I.; Paul, S.; Samantaray, J.C.; Srinivasan, A.; Khalil, S.; Rastogi, N.; Dabas, Y. MALDI-TOF mass spectrometry for rapid identification of clinical fungal isolates based on ribosomal protein biomarkers. *J. Microbiol. Methods* **2015**, *109*, 93–105. [[CrossRef](#)]
37. Newman, D.J.; Cragg, G.M. Natural Products as Sources of New Drugs over the Nearly Four Decades from 01/1981 to 09/2019. *J. Nat. Prod.* **2020**, *83*, 770–803. [[CrossRef](#)]
38. Sadrati, N.; Zerroug, A.; Demirel, R.; Harzallah, D. Anti-multidrug-resistant *Staphylococcus aureus* and anti-dermatophyte activities of secondary metabolites of the endophytic fungus *Penicillium brevicompactum* ANT13 associated with the Algerian endemic plant *Abies numidica*. *Arch. Microbiol.* **2023**, *205*, 110. [[CrossRef](#)] [[PubMed](#)]
39. Wang, X.W.; Bai, F.Y.; Bensch, K.; Meijer, M.; Sun, B.D.; Han, Y.F.; Crous, P.W.; Samson, R.A.; Yang, F.Y.; Houbraken, J. Phylogenetic re-evaluation of *Thielavia* with the introduction of a new family *Podosporaceae*. *Stud. Mycol.* **2019**, *93*, 155–252. [[CrossRef](#)] [[PubMed](#)]
40. Fleming, A. On the antibacterial action of cultures of a *Penicillium*, with special reference to their use in the isolation of *B. influenzae*. *Br. J. Exp. Pathol.* **1929**, *10*, 226–236. [[CrossRef](#)]
41. Chain, E.; Florey, H.; Gardner, A.; Heatley, N.G.; Jennings, M.A.; Orr-Erwing, J.; Sanders, A.G. Penicillin as a chemotherapeutic agent. *Lancet* **1940**, *236*, 226–228. [[CrossRef](#)]
42. Gao, N.; Shang, Z.C.; Yu, P.; Luo, J.; Jian, K.L.; Kong, L.Y.; Yang, M.H. Alkaloids from the endophytic fungus *Penicillium brefeldianum* and their cytotoxic activities. *Chin. Chem. Lett.* **2017**, *28*, 1194–1199. [[CrossRef](#)]
43. Yang, M.H.; Li, T.X.; Wang, Y.; Liu, R.H.; Luo, J.; Kong, L.Y. Antimicrobial metabolites from the plant endophytic fungus *Penicillium* sp. *Fitoterapia* **2017**, *116*, 72–76. [[CrossRef](#)] [[PubMed](#)]
44. Marinho, A.M.; Marinho, P.S.; Filho, E.R. Esteroides produzidos por *Penicillium herquei*, um fungo endofítico isolado dos frutos de *Melia azedarach* (Meliaceae). *Quim. Nova* **2009**, *32*, 1710–1712. [[CrossRef](#)]
45. Koul, M.; Meena, S.; Kumar, A.; Sharma, P.R.; Singamaneni, V.; Hassan, S.R.; Hamid, A.; Chaubey, A.; Prabhakar, A.; Gupta, P.; et al. Secondary metabolites from endophytic fungus *Penicillium pinophilum* induce ROS-mediated apoptosis through mitochondrial pathway in pancreatic cancer cells. *Planta Med.* **2016**, *82*, 344–355. [[CrossRef](#)] [[PubMed](#)]
46. Challinor, V.L.; Bode, H.B. Bioactive natural products from novel microbial sources. *Ann. N. Y. Acad. Sci.* **2015**, *1354*, 82–97. [[CrossRef](#)]
47. Chen, M.; Shen, N.X.; Chen, Z.Q.; Zhang, F.M.; Chen, Y. Penicilones A-D, Anti-MRSA Azaphilones from the Marine-Derived Fungus *Penicillium janthinellum* HK 1-6. *J. Nat. Prod.* **2017**, *80*, 1081–1086. [[CrossRef](#)]
48. Nicoletti, R.; Gresa, L.; Pilar, M.; Manzo, E.; Carella, A.; Ciavatta, M.L. Production and fungitoxic activity of Sch 642305, a secondary metabolite of *Penicillium canescens*. *Mycopathologia* **2007**, *163*, 295–301. [[CrossRef](#)] [[PubMed](#)]

49. Flajs, D.; Peraica, M. Toxicological properties of citrinin. *Arh. Hig. Rada Toksikol.* **2009**, *60*, 457–464. [[CrossRef](#)] [[PubMed](#)]
50. Chang, C.H.; Yu, F.Y.; Wang, L.T.; Lin, Y.S.; Liu, B.H. Activation of ERK and JNK signaling pathways by mycotoxin citrinin in human cells. *Toxicol. Appl. Pharmacol.* **2009**, *237*, 281–287. [[CrossRef](#)] [[PubMed](#)]
51. Nakajima, Y.; Iguchi, H.; Kamisuki, S.; Sugawara, F.; Furuichi, T.; Shinoda, Y. Low doses of the mycotoxin citrinin protect cortical neurons against glutamate-induced. *J. Toxicol. Sci.* **2016**, *41*, 311–319. [[CrossRef](#)] [[PubMed](#)]
52. Hiroyuki, H.; Kensuke, H.; Kozo, S. Mechanism of antifungal action of citrinin. *Agric. Biol. Chem.* **1987**, *51*, 1373–1378. [[CrossRef](#)]
53. Mazumder, P.M.; Mazumder, R.; Mazumder, A.; Sasmal, D.S. Antimicrobial activity of the mycotoxin citrinin obtained from the fungus *Penicillium citrinum*. *Anc. Sci. Life* **2002**, *XXI*, 191–197.
54. Wakana, D.; Hosoe, T.; Itabashi, T.; Okada, K.; de Campos Takaki, G.M.; Yaguchi, T.; Fukushima, K.; Kawai, K.I. New citrinin derivatives isolated from *Penicillium citrinum*. *J. Nat. Med.* **2006**, *60*, 279–284. [[CrossRef](#)]
55. Xu, B.J.; Jia, X.Q.; Gu, L.J.; Sung, C.K. Review on the qualitative and quantitative analysis of the mycotoxin citrinin. *Food Control* **2006**, *17*, 271–285. [[CrossRef](#)]

Disclaimer/Publisher’s Note: The statements, opinions and data contained in all publications are solely those of the individual author(s) and contributor(s) and not of MDPI and/or the editor(s). MDPI and/or the editor(s) disclaim responsibility for any injury to people or property resulting from any ideas, methods, instructions or products referred to in the content.